Research Square

Preprints are preliminary reports that have not undergone peer review.
They should not be considered conclusive, used to inform clinical practice,
or referenced by the media as validated information.

Blood drops to gut maps: dried blood spot metabolomics infers gut microbiome composition and guides probiotic intervention in metabolic disease

Uday Pandey
NISER
Sohini Mukhopadhyay
NISER
Prashanth Dumpuri
MicrobioTx
Kavya S
Axilor
Saurav Patel
MicrobioTx
Abhishek Chinchole
MicrobioTx
Akanksha Gupta
MicrobioTx
Nidhi Mathur
MicrobioTx
Kishore Behera
AIIMS Bhubaneswar
Palok Aich
palok.aich@niser.ac.in

National Institute of Science Education and Research

Article

Keywords:

Posted Date: May 18th, 2026

DOI: https://doi.org/10.21203/rs.3.rs-9134629/v1

License: This work is licensed under a Creative Commons Attribution 4.0 International License.
Read Full License

Additional Declarations: No competing interests reported.

Abstract

Blood metabolomics could offer a minimally invasive route to monitor gut microbiome–host interactions in metabolic disease, but existing serum or plasma approaches are logistically demanding and rarely evaluated in interventional settings. Here we develop and clinically test the Gut Function Test (GFT), a dried blood spot–based LC–MS and elastic-net framework that predicts genus-level gut microbiome composition from systemic metabolites in Indian adults spanning health, obesity and type 2 diabetes. Across 136 genera, GFT achieves 74% confidence-interval accuracy (95% CI 71–77) and Spearman's ρ ≈ 0.75 versus paired stool profiles, with predictive features mapping to branched-chain amino acid, tryptophan–kynurenine, bile-acid and short-chain fatty acid pathways. In an open-label, 3-month trial, cohort-specific probiotics guided by GFT were associated with improved glycaemia in type 2 diabetes and weight loss in obesity, accompanied by GFT-inferred shifts towards beneficial taxa and away from opportunistic Enterobacteriaceae, establishing DBS metabolomics as a scalable tool for microbiome-informed precision interventions.

Introduction

The human gut microbiome is a central determinant of host metabolism, immunity and systemic health, and its disruption has been implicated in obesity, type 2 diabetes (T2D), non-alcoholic fatty liver disease and cardiovascular risk [1,2]. Large cohort studies and mechanistic experiments have established robust associations between gut microbial composition, microbial metabolites and metabolic traits, yet microbiome profiling has had limited impact on routine clinical management of metabolic disease. Decades of research have established robust associations between gut microbial dysbiosis and metabolic disorders, including obesity, type 2 diabetes (T2D), non-alcoholic fatty liver disease, and cardiovascular risk [3–5]. Yet despite these insights and the clear translational potential, the integration of microbiome research into routine clinical practice remains elusive.

A major barrier is methodological: current gold-standard approaches rely on stool-based sequencing, which is inconvenient for patients, logistically demanding for large or repeated sampling and anatomically distal from the systemic compartment where metabolic complications manifest. Stool collection is subject to variability in timing, storage and transport, and sequencing turnaround times can be incompatible with clinical decision-making [6–9]. Moreover, fecal composition provides only a partial, anatomically distal view of the dynamic crosstalk between microbes and the host metabolic environment, failing to capture the functional metabolic outputs that reach systemic circulation [10,11].

Blood, in contrast, offers an integrative and functionally proximal readout of both host and microbial metabolism. Circulating metabolites include microbial fermentation products such as short-chain fatty acids and secondary bile acids, host–microbe co-metabolites such as indoles and trimethylamine N-oxide, and immune-modulating molecules along the kynurenine and serotonin axes [12–14]. Recent work has shown that serum or plasma metabolomic profiles correlate with gut microbiome α-diversity and can predict selected taxa and incident T2D, suggesting that aspects of gut ecology are encoded in the blood

metabolome [15–17]. For example, Menni et al. (2020) showed that serum metabolites reflecting gut microbiome alpha diversity could predict type 2 diabetes risk [15], while Wilmanski et al. (2019) used blood metabolome data to predict microbiome alpha diversity with moderate accuracy [16]. A 2025 Nature Metabolism study in the Framingham cohort identified over 500 blood metabolites associated with impaired glucose control, with approximately one-third linked to an altered gut microbiome, demonstrating that the gut microbiota account for nearly 30% of blood metabolite variance in prediabetes and T2D, twice that observed in healthy individuals [18]. However, these studies have several limitations for translation [15]. They typically use liquid blood requiring venepuncture and cold-chain logistics, restricting scalability for longitudinal or community-based monitoring [16]. Most focus on global diversity or risk scores rather than taxon-resolved composition, and few, if any, have been evaluated as tools to guide or track microbiome-targeted interventions. However, most prior approaches remain exploratory, use liquid blood samples requiring cold-chain logistics, lack robust validation metrics with clinical interpretability, and critically, have not been validated in interventional contexts to demonstrate clinical utility [15,16,18,19]. There is therefore a pressing need for robust, scalable, logistically feasible, and clinically actionable methods to infer microbiome composition from blood-based metabolomics data.

Dried blood spot (DBS) sampling could overcome many of these constraints. DBS collection via finger-stick is minimally invasive, requires no specialized infrastructure, and cards can be shipped and stored at ambient temperature with good analytical stability for hundreds of metabolites [20–22]. These properties have led to increasing use of DBS in newborn screening and population-scale metabolomics, but DBS-based assays have not yet been leveraged to infer gut microbiome composition or to support microbiome-informed therapy in metabolic disease [23,24]. More broadly, there is a need for frameworks that couple interpretable machine-learning models with uncertainty-aware metrics so that blood-derived microbiome surrogates can be meaningfully deployed in clinical decision pathways.

Here we introduce the Gut Function Test (GFT), a DBS-based, untargeted LC–MS and elastic-net modelling platform that predicts genus-level gut microbial abundances from systemic metabolites and evaluates its performance in both observational and interventional settings. Using paired stool and DBS samples from Indian adults who are healthy, obese or have T2D, we train and benchmark GFT across 136 genera, quantify prediction performance with a clinically interpretable confidence-interval accuracy metric and map key metabolite predictors onto canonical metabolic pathways. We then test whether GFT can track microbiome-targeted intervention in an open-label, cohort-specific probiotic trial in obesity and T2D, relating GFT-inferred microbial shifts to changes in glycaemic control and body weight. This work establishes a minimally invasive blood-based approach to microbiome phenotyping and provides a generalizable template for integrating metabolomics, machine learning and targeted interventions in human metabolic disease [18].

We benchmark GFT using paired DBS and stool samples from three Indian cohorts (healthy controls, obesity, and T2D), evaluating predictive accuracy across genera, cohorts, and individuals. We demonstrate that metabolite-based predictions achieve 74% CI accuracy (95% CI: 71–77%) with strong

Spearman correlations (ρ ≈ 0.75) to stool-derived 16S rRNA sequencing profiles. We validate the biological plausibility of metabolite–microbe associations by mapping predictive features to established metabolic pathways, including branched-chain amino acid (BCAA) metabolism, tryptophan–kynurenine signaling, and short-chain fatty acid (SCFA) production [25–29].

Critically, we demonstrate proof-of-concept clinical validation through a 3-month, open-label intervention study. Cohort-specific probiotic formulations targeting predicted microbial deficiencies led to significant improvements in glycaemia (fasting blood glucose declined by 26% at 2 months in T2D) and body weight (8% reduction over 3 months in obesity), with GFT-predicted microbiome rebalancing aligning temporally and functionally with observed metabolomic shifts. While the open-label design precludes definitive efficacy conclusions and larger randomized controlled trials are essential, this proof-of-concept provides initial evidence that GFT can guide and monitor microbiome-targeted therapeutic interventions.

Taken together, this work establishes GFT as a scalable, reproducible, and clinically interpretable approach to blood-based microbiome profiling. By enabling minimally invasive inference of microbial composition with transparent validation metrics and demonstrated biological plausibility, GFT addresses a major translational barrier, opening new avenues for precision health, longitudinal microbiome monitoring, and microbiome-guided therapeutic decision-making in metabolic disease management.

Results

Cohort characteristics and baseline microbiome diversity

In Phase 1, we profiled 76 adults (healthy control, obese, and type 2 diabetes [T2D] cohorts) who provided paired stool and fingerstick blood samples (Table 1; Table S1). The groups were broadly comparable in age and sex, but—as expected—the obese and T2D cohorts had significantly higher BMI, waist circumference, fasting glucose, and HbA1c than controls. For example, mean BMI was ∼30 in obese and ∼28 in T2D versus ∼22 in controls ($p < 0.001$), and median HbA1c was above diabetes threshold only in the T2D group (Table S1). These differences reflect the metabolic status of each group.

We next examined the gut microbiome diversity across cohorts. Alpha diversity (measured by Shannon index, Simpson index, and observed genus richness) was highest in healthy controls and progressively lower in the obese and T2D groups (Fig. S1). In other words, controls harbored a richer and more even gut community, whereas obesity was associated with a moderate decline, and T2D with an even further reduction in diversity. This stepwise loss of diversity suggests that microbial dysbiosis correlates with metabolic disease severity. Consistent with this, individual variability (outliers) was present in all groups, reflecting normal inter-subject differences in microbiomes.

Beta diversity analysis (principal coordinates analysis, Bray–Curtis dissimilarity) also revealed cohort-specific patterns. Control samples clustered relatively tightly in ordination space, indicating a more uniform community structure, whereas obesity and T2D samples were more dispersed (Fig. S2). The clusters of the three groups overlapped partially, indicating that some taxa were shared across cohorts,

but each group occupied a distinct region of the plot. In particular, the T2D cohort showed the greatest spread, suggesting high inter-individual variability and substantial shift in community composition relative to controls. The overall pattern implies that progression from healthy to obese to T2D is accompanied by systematic microbiome shifts, rather than an entirely random change.

Gut Function Test (GFT) model development and benchmarking

We developed the Gut Function Test by training genus-level Elastic Net regression models to predict gut microbial abundances from blood metabolomic profiles. All available blood metabolites (after data cleaning and imputation) were included as predictors (no explicit pre-filtering of metabolites was applied). In total, 136 genus models were trained using paired stool (16S) and dried blood spot metabolomics from the 76 Phase 1 subjects. Missing metabolite values were replaced with the median (per metabolite) and each metabolite profile was z-scored to ensure comparable scaling (see Methods). We used 10-fold cross-validation on the training set to optimize the elastic-net mixing (α) and regularization (λ) parameters. No special stratification or grouping was enforced (i.e. the folds were random splits, treating all samples as independent), since each genus model was trained independently and the response variable was continuous.

Model performance was assessed by conventional metrics (Spearman correlation, R^2) and by our clinically interpretable CI accuracy metric, defined as the fraction of predictions that fall within the empirically observed 95% abundance interval of each genus. Across all models and cohorts, the mean CI accuracy was ~ 74%. In other words, on average three quarters of genus predictions were within the native abundance range observed in stools. The Spearman correlation between predicted and observed abundances was also strong ($\rho \approx 0.75$, $p \ll 0.001$). Importantly, over 40% of genera achieved ≥ 90% CI accuracy, demonstrating that many taxa were predicted very precisely. For example, the mucin-degrader *Akkermansia* and the butyrate-producer *Butyrivibrio* were among the best-predicted genera (often with > 95% CI accuracy), whereas genera like *Prevotella* and *Megasphaera* were less accurately inferred (typically ~ 60–70% CI accuracy). Figure 1e summarizes these results: it shows the distribution of CI accuracy across all genera in each cohort, highlighting the high- and low-performing taxa.

Model performance was robust. Bootstrap resampling produced similar accuracy distributions (data not shown), and an independent 20% hold-out set (external test) gave comparable results, indicating minimal overfitting. We also examined model generalization to new cohorts: training on combined data from all three groups yielded similar accuracy to cohort-specific training, implying that the metabolic signatures of each genus are largely preserved across these populations.

To further validate the models, we performed pathway enrichment on the top predictive metabolites (Fig. 2d). The enriched pathways were biologically coherent: amino acid metabolism (especially branched-chain and aromatic amino acids), tryptophan–kynurenine metabolism, and short-chain fatty acid (SCFA) biosynthesis emerged as top hits. For example, elevated kynurenine levels (tryptophan breakdown) were linked to increased abundance of pro-inflammatory taxa, whereas higher serotonin

(another tryptophan product) was associated with beneficial genera (consistent with host–microbiome neuroimmune regulation). These pathway findings (colored by category in Fig. 2d) mirror known axis of dysbiosis in obesity/T2D. Together, the high CI accuracies and the biological relevance of the top features demonstrate that GFT is capturing meaningful, reproducible relationships between the blood metabolome and gut microbiome composition.

Supplementary analyses support these conclusions. A genus-wise breakdown of CI accuracy (Fig. S3) shows that prediction quality varies by taxon, but most common gut microbes are well-inferred. We also verified that no strong batch effects or analytical artifacts biased the results: metabolite quality-control samples showed low variance (most CV% < 10%; Fig. S4), and principal components of the metabolomics data separated cohorts rather than analytical batches. In summary, the GFT achieves ~ 74% predictive accuracy on held-out data, with many genera predicted with > 90% accuracy, and the models rely on metabolite signals that are mechanistically linked to microbial activity.

Metabolite–microbe association patterns by cohort

To visualize how the metabolite–microbe relationships change with metabolic status, we constructed heatmaps of the top 50 metabolite–genus associations for each cohort (Fig. S5). In the healthy controls, the map was sparse and structured: only a few genera showed consistent associations, and the patterns were largely uni-directional. For example, *Weissella*, *Streptococcus*, and *Lactobacillus* each had a handful of positive associations with certain metabolites, reflecting stable fermentative niches in a balanced gut. This limited, genus-specific signature likely reflects well-regulated metabolic interactions in health.

By contrast, the obese cohort's heatmap was more heterogeneous. A broader set of genera became prominent, including *Bilophila*, *Megasphaera*, *Flavonifractor*, *Klebsiella*, and *Oscillibacter*, each strongly associated with multiple metabolites. The number and magnitude of significant associations roughly doubled compared to controls. Notably, several genera exhibited bidirectional associations (both strong positive and negative links), indicating context-dependent interactions. For instance, *Bilophila* was positively correlated with certain lipid metabolites but negatively with others, suggesting altered bile-acid metabolism in obesity. The emergent pattern suggests that obesity involves a reorganization of host–microbe crosstalk – not a loss of all structure, but a shift toward a more complex and perturbed network.

In T2D, the perturbation was most extreme. The associations clustered into concentrated blocks dominated by a few taxa: *Klebsiella*, *Escherichia–Shigella*, *Gemmiger*, *Roseburia*, and *Sphingomonas* had the strongest links. The heatmap for T2D showed marked red-and-blue blocks, indicating both strong positive and negative correlations (often >|0.5|). These taxa were scarcely involved in the control network, highlighting a disease-specific signature. Many of the T2D-associated metabolites were related to amino-acid catabolism, xenobiotic degradation, and lipid pathways. For example, increases in certain amino-acid metabolites aligned with *Escherichia–Shigella*, while decreases in SCFA precursors aligned with the loss of *Roseburia*. In sum, T2D exhibited a qualitative shift: new association patterns appeared

(absent in health), and existing ones became amplified or reversed. This indicates a loss of metabolic resilience and a decoupling of the normal host–microbiome interactions in advanced dysbiosis.

These cohort-specific maps underscore the biological plausibility of GFT. The identified metabolite drivers (BCAAs, bile acids, SCFAs, tryptophan derivatives, etc.) and affected genera (pathogens vs. commensals) are consistent with known microbiome contributions to metabolic disease. Moreover, the shifting network from Controls→Obesity→T2D (i.e. sparse → heterogeneous → extreme) mirrors the clinical progression: obesity represents an intermediate dysbiosis that becomes more pronounced in T2D. These findings reinforce that GFT is not only predictive but also reflects mechanistic biology. As an example, *Klebsiella* and *Escherichia–Shigella* (opportunistic Enterobacteriaceae) showed strong positive associations with metabolites of amino-acid metabolism in T2D (Fig. S8), aligning with their known expansion in diabetic gut and roles in endotoxin-mediated inflammation.

Cohort-specific probiotic intervention (Phase 2)

To test whether GFT could track microbiome changes during treatment, we conducted an open-label 3-month trial in which 53 adults with obesity or T2D received cohort-specific probiotic formulations. Each formulation contained 8 strains chosen for metabolic relevance (e.g. *Bifidobacterium longum*, *Lactobacillus plantarum*, *Streptococcus thermophilus*). We analyzed the 24 participants (12 obese, 12 T2D) who completed at least two follow-up visits. Clinical and molecular measurements were taken at baseline and monthly for 3 months.

Clinical outcomes. The primary clinical endpoints were glucose control (T2D) and body weight (obesity). Figure 3a–d shows the trajectories for fasting blood glucose (FBG), postprandial glucose (PPBG), HbA1c (T2D only), and weight. In the T2D cohort, mean FBG decreased by ~ 26% relative to baseline by month 2 ($p < 0.05$ vs. baseline) and remained stable through month 3 (Fig. 3a). PPBG dropped by ~ 40% by month 3 ($p < 0.01$ vs. baseline) (Fig. 3b). Consequently, mean glycemia improved markedly; the majority of individuals showed downward trends in both FBG and PPBG (see individual points in Fig. 3a–b). HbA1c exhibited a smaller decline (~ 0.5% absolute drop) over 3 months (Fig. 3c); this change was not statistically significant in our small sample, but qualitatively consistent with improved glycemic control. In the obesity cohort, mean body weight fell by ~ 8% by month 3 (from 85 kg to 78 kg, $p < 0.01$ vs. baseline) (Fig. 3d). Secondary measures (waist circumference, BMI) showed corresponding reductions (data not shown).

All group comparisons to baseline were assessed by repeated-measures ANOVA with Dunnett's test. Asterisks in Fig. 3a–d denote significance (*$p < 0.05$; **$p < 0.01$). We specifically ensured that baseline values were explicitly included as the reference in these analyses. By month 3, the reductions in FBG and PPBG (T2D) and in weight (obesity) were statistically significant (Fig. 3a–d). Notably, each plot in Fig. 3 (a–d) overlays individual data points on the boxplot/IQR summary, highlighting inter-individual variability. Some subjects experienced larger improvements than others, but the overall trend in each cohort was an improvement. Fig. S6 shows "spaghetti plots" of these trajectories for each subject: T2D participants

generally show consistent downward trends in FBG, PPBG, HbA1c and weight (despite some noise), whereas obesity patients showed modest declines in FBG/PPBG and mild weight loss (with HbA1c stable).

Predicted microbiome changes. We applied GFT to the DBS samples collected before (month 0) and after the intervention (month 3). The predicted gut microbiome profiles revealed net shifts towards a healthier composition. As one summary, Fig. 3e plots the predicted ratio of "harmful-to-beneficial" genera for each individual, before and after treatment. This ratio significantly declined post-intervention (median drop from ~ 1.2 to ~ 0.7, $p < 0.01$). In other words, the model predicts an increase in SCFA-producing/commensal taxa relative to pathogens.

Figure 3f shows the effect sizes (Cohen's *d*) for selected genera. Consistent with the ratio metric, we observed large positive *d* values for beneficial taxa (indicating increased abundance) and large negative *d* values for pathogenic taxa (indicating decreased abundance). For example, *Butyrivibrio* and *Akkermansia* (both SCFA-producers) had + $d \approx 1.0–1.2$, whereas *Klebsiella* and *Escherichia–Shigella* had − $d \approx 1.0–1.5$. These represent large shifts. The changes in *d* align with known probiotic effects: our formulations were expected to boost commensals and suppress pathobionts. All effect sizes were computed by paired t-test (two-sided), and the genera shown in Fig. 3f passed a nominal significance threshold ($p < 0.05$) before multiple-test correction.

Finally, we explored whether the predicted microbiome improvement correlated with clinical outcomes. Figure 3g plots the per-subject change in the harmful/beneficial ratio against the corresponding change in a clinical metric (e.g. weight loss in the obese, or HbA1c reduction in T2D). There was a clear trend: individuals with larger predicted microbiome rebalancing tended to have greater metabolic improvements. For instance, the correlation coefficient between microbiome ratio changes and percent weight loss was about $R \approx -0.5$ ($p < 0.05$), suggesting that more "healthy-shifted" microbiomes accompanied larger weight reductions. This relationship did not reach formal statistical power in our small trial, but it supports the clinical relevance of the GFT predictions.

In summary, the probiotic intervention produced measurable clinical benefits (improved glycemic control in T2D, weight loss in obesity) and concurrent changes in the inferred microbiome. Predicted increases in beneficial SCFA-producing genera and decreases in pathogens were consistent with the metabolomic shifts we observed (e.g. declines in BCAAs and aromatic amino acids and rises in glycine and SCFA-related compounds; data not shown). These results demonstrate proof-of-concept that GFT not only predicts baseline microbiome composition but can also detect directional changes in response to therapy.

Collectively, our updated analyses (supported by Fig. S1–S6) show that the Gut Function Test performs robustly and in a clinically interpretable manner. It achieves high predictive accuracy for the gut microbiome from blood metabolites, identifies biologically meaningful metabolite–microbe links, and captures microbiome rebalancing during intervention. This positions the GFT as a potentially useful tool for an almost non-invasive microbiome monitoring in metabolic disease.

Discussion

The gut microbiome is tightly linked to metabolic disease, yet translation into clinical practice has been hampered by reliance on stool sequencing, which is inconvenient, logistically demanding and anatomically distal from systemic host–microbe interactions. Blood metabolomics provides a more proximal readout of co-metabolism, and several large cohorts have shown that circulating metabolites correlate with gut microbiome diversity and predict incident metabolic disease[30–32]. Menni et al. and Wilmanski et al. reported that specific serum or plasma metabolites explain a substantial fraction of microbiome α-diversity and forecast type 2 diabetes (T2D) risk, and that the microbiome accounts for a notable proportion of blood metabolite variance. However, these approaches typically use liquid blood requiring venepuncture and cold-chain handling, focus on global diversity rather than taxon-resolved composition, and have not been evaluated as tools to guide or monitor interventions. Our study addresses this gap by introducing the Gut Function Test (GFT), a dried blood spot (DBS)–based untargeted LC–MS and machine-learning platform that infers genus-level gut microbial composition and tracks microbiome-targeted therapy in obesity and T2D.

By integrating DBS metabolomics with elastic-net models, we show that systemic metabolites can recover a large fraction of inter-individual variability in stool-derived genus abundances, achieving a mean confidence-interval (CI) accuracy of 74% and a Spearman's ρ of about 0.75 across three Indian cohorts spanning health, obesity and T2D. More than 40% of genera are predicted with ≥90% CI accuracy, including canonical mucin degraders and short-chain-fatty-acid (SCFA) producers such as *Akkermansia* and *Butyrivibrio*, whereas genera with known context-dependent ecology, such as *Prevotella*, are less accurately inferred. The CI accuracy metric explicitly embeds uncertainty by asking whether a predicted abundance falls within the empirically observed 95% interval for each genus, providing a clinically interpretable complement to correlation coefficients. This uncertainty-aware framing is particularly important for prospective decision-making, where approximate ranking within a physiological range may be more actionable than exact point estimates. Consistent with extensive literature linking reduced microbial diversity and compositional shifts to metabolic disease, we observed stepwise reductions in α-diversity and coherent shifts in β-diversity from controls to obesity to T2D, supporting the use of metabolite-encoded microbial information as a quantitative readout of dysbiosis severity[30–35].

The metabolite features that drive GFT predictions map onto metabolic axes with established roles in metabolic disease. Elevated branched-chain amino acids and aromatic amino-acid catabolites positively associate with opportunistic Enterobacteriaceae, including Escherichia–Shigella and Klebsiella, consistent with their expansion in insulin resistance and T2D and with prior multi-omics analyses linking these metabolites to dysbiosis and inflammation. Conversely, bile-acid derivatives and SCFA-related substrates are enriched as predictors for beneficial genera such as *Butyrivibrio*, *Roseburia* and *Agathobacter*, aligning with their recognized roles in maintaining gut barrier integrity and metabolic homeostasis. Cohort-stratified association maps show a progression from a relatively sparse, structured network in healthy individuals to a more heterogeneous, rewired configuration in obesity and a highly polarized pattern in T2D dominated by a few pathobionts and depleted commensals. These qualitative

shifts mirror the loss of resilience and emergence of disease-specific host–microbe circuits described in other multi-omics studies and suggest that blood-encoded signatures can resolve not only the magnitude but also the architecture of dysbiosis.[32,35,36].

A distinctive aspect of this work is the proof-of-concept clinical validation of a blood-based microbiome test in an interventional setting. In a 3-month, open-label trial, cohort-specific multi-strain probiotics were selected to address predicted deficits in SCFA-producing and barrier-supporting taxa in individuals with obesity or T2D. The intervention was associated with significant reductions in fasting and post-prandial glycaemia in T2D and an approximate 8% decrease in body weight in obesity, accompanied by a decline in a GFT-derived harmful-to-beneficial genus ratio and large Cohen's d effect sizes for key genera: increases in *Akkermansia* and *Butyrivibrio* and decreases in *Klebsiella* and *Escherichia–Shigella*. Participants exhibiting larger GFT-predicted microbiome rebalancing tended to show greater improvements in glycaemia or weight, supporting the biological and clinical relevance of the inferred shifts, although the study was not powered to establish formal mediation. Together, these findings indicate that DBS metabolomics can be used not only to approximate baseline microbiome composition but also to sensitively detect directional change in response to therapy [30–32,34,37,38].

DBS sampling is central to the translational potential of GFT. Finger-stick collection eliminates the need for venepuncture and cold-chain logistics, facilitates mail-in sampling and repeated measurements, and is compatible with large-scale community or resource-limited settings. Previous analytical work has shown that hundreds of metabolites remain stable for prolonged periods on DBS cards and correlate well with paired plasma measurements, supporting their suitability for clinical and epidemiological applications. By coupling this practical matrix with an interpretable machine-learning framework, GFT provides a scalable route to blood-based microbiome phenotyping that could be embedded into existing screening programmes or therapeutic monitoring pathways challenging[17,18,30–34,37,39,40].

This study has several limitations. Predictions are constrained to the genus level and rely on 16S rRNA–based taxonomic profiles rather than shotgun metagenomes, precluding detailed functional inference at the strain level. The intervention was open-label, with modest sample size and no placebo arm, so regression to the mean, behaviour change or other unmeasured factors may contribute to the observed clinical improvements. Diet, medication and other exposures that modulate both metabolites and microbes were not exhaustively controlled, and our models, while robust across cohorts in this setting, will require re-calibration in other populations and disease contexts [30–33,38].

Future work should integrate GFT with metagenomic and meta-transcriptomic data, evaluate causal relationships via randomized controlled trials and perturbation experiments, and explore non-linear or multi-task learning strategies for joint prediction of consortia and pathways [30,32,33,35,38].

Despite these caveats, our findings demonstrate that a minimally invasive DBS-based metabolomics assay can infer gut microbiome composition with high accuracy, recapitulate mechanistic host–microbe pathways and monitor microbiome-directed intervention in metabolic disease [32,35,36,38]. GFT provides a

generalizable framework for leveraging systemic metabolite profiles as a surrogate for intestinal ecological state, and could be adapted to other indications where the gut microbiome modulates extra-intestinal physiology, including immunotherapy response, neuropsychiatric disorders and chronic inflammation [30,32,34,35]. As such, this work moves blood-based microbiome research from cross-sectional association towards a clinically interpretable, interventional paradigm [30,32,35,36,38].

Online Methods

Study design, ethics, and participants

The study consisted of Phase 1 (paired stool–DBS profiling) and Phase 2 (open-label probiotic intervention). Ethics approvals in accordance with the Declaration of Helsinki were obtained from AIIMS Bhubaneswar (Ref. T/EM-F/Endocri/21/75) and NISER (IEC NISER/IEC/2023-01). This study is registered with the Clinical Trials Registry (CTRI), India on 23/08/2022 with the following reference number: REF/2022/08/057600 prior to the commencement of the study. Written informed consent was obtained from all participants. Inclusion criteria defined obesity as BMI ≥25 kg m^{-2} and T2D as HbA1c >6.4%. Phase 1 enrolled 76 adults (healthy, obese, and T2D). Phase 2 enrolled 53 adults; participants with ≥2 post-baseline timepoints (n = 12 per cohort) were included in longitudinal analyses.

Sample collection and clinical measurements

Stool was self-collected in sterile containers, transported on a cold chain, and stored at −80 °C. Fingerstick blood was spotted onto Whatman DBS cards, air-dried, and stored at 4 °C with a desiccant. For Phase 2, samples and clinical measures—FBG, PPBG, HbA1c, and weight—were obtained at baseline and at 1, 2, and 3 months; adverse events were monitored at bi-weekly calls.

Fecal DNA extraction and 16S rRNA sequencing

Genomic DNA was extracted from ~200 mg of stool using the QIAamp Fast DNA Stool Mini Kit (Qiagen). DNA integrity and quantity were assessed by Nanodrop and Qubit. The V3–V4 region was amplified (341F/805R) and sequenced on an Ion GeneStudio S5 (Ion 530 chip). Reads were processed with the Ion Reporter pipeline to generate genus-level abundance tables. Analyses focused on relative abundances at the genus level for robustness.

Untargeted metabolomics from dried blood spots

Five 3-mm punches per DBS were extracted in 1:1 methanol: acetonitrile (0.1% formic acid) containing internal standards. Extracts were gently agitated (2 h, RT), precipitated (4 °C, 2 h), centrifuged (16,000 g, 15 min, 4 °C), dried (vacuum), and reconstituted in 1:1 acetonitrile: water. LC–MS employed a Kinetex C18 column (2.6 µm, 100 mm × 4.6 mm) with mobile phases A (water, 0.1% formic acid) and B (acetonitrile, 0.1% formic acid), 20-min gradient, 5-µL injection. An AB Sciex TripleTOF 6600, operated in positive/negative ESI mode, acquired data-dependent MS/MS. Features were deconvoluted and aligned

in MS-DIAL v4.9[41]; metabolites were annotated against spectral libraries, including HMDB 5.0. Metabolites[42] were assigned origin (host vs. microbial) using MetOrigin and chemical classes using HMDB taxonomy.

Machine learning model: Gut Function Test (GFT)

Metabolite matrices and genus abundance tables were converted to relative abundances; metabolites were z-scored; and missing values were imputed by median. For each genus, an ElasticNet regressor (scikit-learn) was used to model abundance based on metabolite features.[43] To enhance clinical interpretability, we defined CI accuracy as a prediction being correct if it fell within the 95% observed abundance interval for that genus in the training data. Furthermore, we report the fraction of genera with ≥90% CI accuracy. Code implements deterministic splits and fixed random seeds to ensure reproducibility.

Pathway and statistical analysis

Differential metabolite patterns were summarized by effect sizes (Cohen's d) (Fig. 3f).[44] Pathway over-representation and topology were assessed in MetaboAnalystR 4.0 using KEGG (hypergeometric test; betweenness centrality).[45] Clinical trajectories were analyzed by repeated-measures one-way ANOVA (mixed effects) with Dunnett's correction versus baseline. Two-sided $\alpha < 0.05$ was considered significant. Scripts (R 4.3; Python 3.10) are provided.

Probiotic formulations and administration

Cohort-specific formulations (8×10^9 CFU per capsule) were administered once daily before breakfast for three months. T2D: *Bifidobacterium infantis, B. breve, B. lactis, B. longum, Lactobacillus rhamnosus, L. paracasei, L. plantarum, Streptococcus thermophilus; Obesity: Lactobacillus gasseri, L. acidophilus, L. rhamnosus, L. fermentum, B. longum, L. plantarum, S. thermophilus, L. bulgaricus*. Both included fructo-oligosaccharide as a prebiotic. No serious adverse events were observed.

Declarations

Competing interests

The authors declare no competing interests.

Author Contribution

U.P. and S.M. recruited participants, collected samples, performed experiments and analyzed data. P.D. designed and implemented the GFT models and performed computational analyses. K.S. assisted in finalizing the manuscript by critical reading suggestions and rewriting. S.P. and A.C. assisted with

analytics and data processing. A.G., N.M. provided critical comments and suggestions. K.B. provided clinical oversight and interpretation. P.A. conceived and supervised the study, secured funding, structured, drafted and finalized the manuscript. All authors approved the final version.

Acknowledgements

We thank all participants. This work was supported by a grant by Axilor Ventures Pvt. Ltd. (Bengaluru) and by providing infrastructural facility by NISER (DAE, Government of India).

Data Availability

De-identified metabolomics matrices, genus tables, and analysis outputs are available at: [https://github.com/MicrobioTx/ProbioticsClinicalTrialPaper] (https:/github.com/MicrobioTx/ProbioticsClinicalTrialPaper) . 16S reads and metadata will be provided upon reasonable request to the corresponding author after institutional approval. All analysis code (preprocessing, modeling, statistics, and figure generation) is provided in the same repository.

References

1. Nicholson, J. K. *et al.* Host-gut microbiota metabolic interactions. *Science (1979)*. 336, 1262–1267 (2012).
2. Zhang, H. *et al.* Microbiota, chronic inflammation, and health: The promise of inflammatome and inflammatomics for precision medicine and health care. *hLife* 3, 307–326 (2025).
3. Visconti, A. *et al.* Interplay between the human gut microbiome and host metabolism. *Nat. Commun.* 10, (2019).
4. Sasidharan Pillai, S., Gagnon, C. A., Foster, C. & Ashraf, A. P. Exploring the gut microbiota: key insights into its role in obesity, metabolic syndrome, and type 2 diabetes. *Journal of Clinical Endocrinology and Metabolism* 109, 2709–2719 (2024).
5. Madhogaria, B., Bhowmik, P. & Kundu, A. Correlation between human gut microbiome and diseases. *Infect. Dis. Model.* 7, 448–460 (2022).
6. Kopparam, P. *et al.* From burden to hope: Noncommunicable diseases in India and the gut microbiome. *iMeta* 3, e211 (2024).
7. Nearing, J. T., Comeau, A. M. & Langille, M. G. I. Identifying biases and their potential solutions in human microbiome studies. *Microbiome* 9, (2021).
8. Altamirano, J., Saa, P. A. & Garrido, D. Inferring composition and function of the human gut microbiome in time and space: A review of genome-scale metabolic modelling tools. *Comput. Struct. Biotechnol. J.* 18, 3897–3904 (2020).
9. Van Hul, M. *et al.* What defines a healthy gut microbiome? *Gut* 73, 1893–1908 (2024).

10. de Vos, W. M., Tilg, H., Van Hul, M. & Cani, P. D. Gut microbiome and health: mechanistic insights. *Gut* 71, 1020–1032 (2022).
11. Zhang, Y., Chen, R., Zhang, D. D., Qi, S. & Liu, Y. Metabolite interactions between host and microbiota during health and disease: Which feeds the other? *Biomedicine and Pharmacotherapy* 160, 114295 (2023).
12. Khan, I. *et al.* Integrated analysis of blood microbiome and metabolites reveals key biomarkers and functional pathways in myocardial infarction. *J. Transl. Med.* 23, 31 (2025).
13. Liu, X. *et al.* Mendelian randomization analyses support causal relationships between blood metabolites and the gut microbiome. *Nat. Genet.* 54, 52–61 (2022).
14. Li, K., Naviaux, J. C., Bright, A. T., Wang, L. & Naviaux, R. K. A robust, single-injection method for targeted, broad-spectrum plasma metabolomics. *Metabolomics* 13, 54 (2017).
15. Menni, C. *et al.* Serum metabolites reflecting gut microbiome alpha diversity predict type 2 diabetes. *Gut Microbes* 11, 1632–1642 (2020).
16. Wilmanski, T. *et al.* Blood metabolome predicts gut microbiome ?-diversity in humans. *Nat. Biotechnol.* 37, 1217–1228 (2019).
17. Lokhov, P. G., Kharybin, O. N. & Archakov, A. I. Linking clinical blood metabogram and gut microbiota. *Metabolites* 13, 1096 (2023).
18. Li, J. *et al.* Microbiome□metabolome dynamics associated with impaired glucose homeostasis. *Nat. Metab.* 7, 684–701 (2025).
19. Mallick, H. *et al.* Predictive metabolomic profiling of microbial communities using amplicon or metagenomic sequences. *Nat. Commun.* 10, (2019).
20. Francke, M. I. *et al.* Best practices to implement dried blood spot sampling for therapeutic drug monitoring in clinical practice. *Ther. Drug Monit.* 45, 43–55 (2023).
21. Chepyala, D. *et al.* Improved dried blood spot-based metabolomics analysis by a postcolumn infused-internal standard assisted LC□ESI-MS method. *Anal. Chem.* 91, 10702–10712 (2019).
22. Chen, J. *et al.* Utilization and validation of dried blood spot-based metabolomics for screening metabolic syndrome. *Microchemical Journal* 206, 111522 (2024).
23. Xie, J. *et al.* Improved metabolite prediction using microbiome data-based elastic net models. *bioRxiv* https://doi.org/10.1101/2021.07.01.450697 (2021) doi:10.1101/2021.07.01.450697.
24. Marzougui, A., Ma, Y., McGee, R. J., Khot, L. R. & Sankaran, S. Generalized linear model with elastic net regularization and convolutional neural network for evaluating aphanomyces root rot severity in lentil. *Plant Phenomics* 3075934 (2020) doi:10.34133/2020/3075934.
25. Agus, A., Planchais, J. & Sokol, H. Gut microbiota regulation of tryptophan metabolism in health and disease. *Cell Host Microbe* 23, 716–724 (2018).
26. Blaak, E. E. *et al.* Short chain fatty acids in human gut and metabolic health. *Benef. Microbes* 11, 411–455 (2020).

27. Gojda, J. & Cahova, M. Gut microbiota as the link between elevated BCAA serum levels and insulin resistance. *Biomolecules* 11, 1414 (2021).
28. Derrien, M., Belzer, C. & de Vos, W. M. Akkermansia muciniphila and its role in regulating host functions. *Microb. Pathog.* 106, 171–181 (2017).
29. Chandel, N. *et al.* Characterisation of Indian gut microbiome for B-vitamin production and preliminary assessment of B-vitamin status. *British Journal of Nutrition* 131, 575–590 (2024).
30. Wilmanski, T. *et al.* Blood metabolome predicts gut microbiome α-diversity in humans. *Nat. Biotechnol.* 37, 1217–1228 (2019).
31. Menni, C. *et al.* Serum metabolites reflecting gut microbiome alpha diversity predict type 2 diabetes. *Gut Microbes* 11, 1632–1642 (2020).
32. Visconti, A. *et al.* Interplay between the human gut microbiome and host metabolism. *Nat. Commun.* 10, (2019).
33. DeBalsi, K. L. *et al.* Dried blood spots capture a wide range of metabolic pathways and biological changes associated with exercise. *Metabolomics* 22, (2025).
34. Tobin, N. H. *et al.* Comparison of dried blood spot and plasma sampling for untargeted metabolomics. *Metabolomics* 17, (2021).
35. Cui, H. N. *et al.* Evaluation of metabolite stability in dried blood spot stored at different temperatures and times. *Sci. Rep.* 14, (2024).
36. Dekkers, K. F. *et al.* An online atlas of human plasma metabolite signatures of gut microbiome composition. *Nat. Commun.* 13, (2022).
37. Zhu, T. & Goodarzi, M. O. Metabolites Linking the Gut Microbiome with Risk for Type 2 Diabetes. *Curr. Nutr. Rep.* 9, 83–93 (2020).
38. Chiu, H. H. *et al.* A comparative study of plasma and dried blood spot metabolomics and its application to diabetes mellitus. *Clinica Chimica Acta* 552, (2024).
39. Sasidharan Pillai, S., Gagnon, C. A., Foster, C. & Ashraf, A. P. Exploring the Gut Microbiota: Key Insights Into Its Role in Obesity, Metabolic Syndrome, and Type 2 Diabetes. *J. Clin. Endocrinol. Metab.* 109, 2709–2719 (2024).
40. Li, K., Naviaux, J. C., Monk, J. M., Wang, L. & Naviaux, R. K. Improved dried blood spot-based metabolomics: A targeted, broad-spectrum, single-injection method. *Metabolites* 10, 82 (2020).
41. Tsugawa, H. *et al.* MS-DIAL: Data-independent MS/MS deconvolution for comprehensive metabolome analysis. *Nat. Methods* 12, 523–526 (2015).
42. Wishart, D. S. *et al.* HMDB 5.0: The Human Metabolome Database for 2022. *Nucleic Acids Res.* 50, D622–D631 (2022).
43. Xie, J. *et al.* Improved Metabolite Prediction Using Microbiome Data-Based Elastic Net Models. Preprint at https://doi.org/10.1101/2021.07.01.450697 (2021).
44. Cohen, J. *Statistical Power Analysis for the Behavioral Sciences Second Edition*.

45. Pang, Z. *et al.* MetaboAnalystR 4.0: a unified LC-MS workflow for global metabolomics. *Nat. Commun.* 15, (2024).

Figures

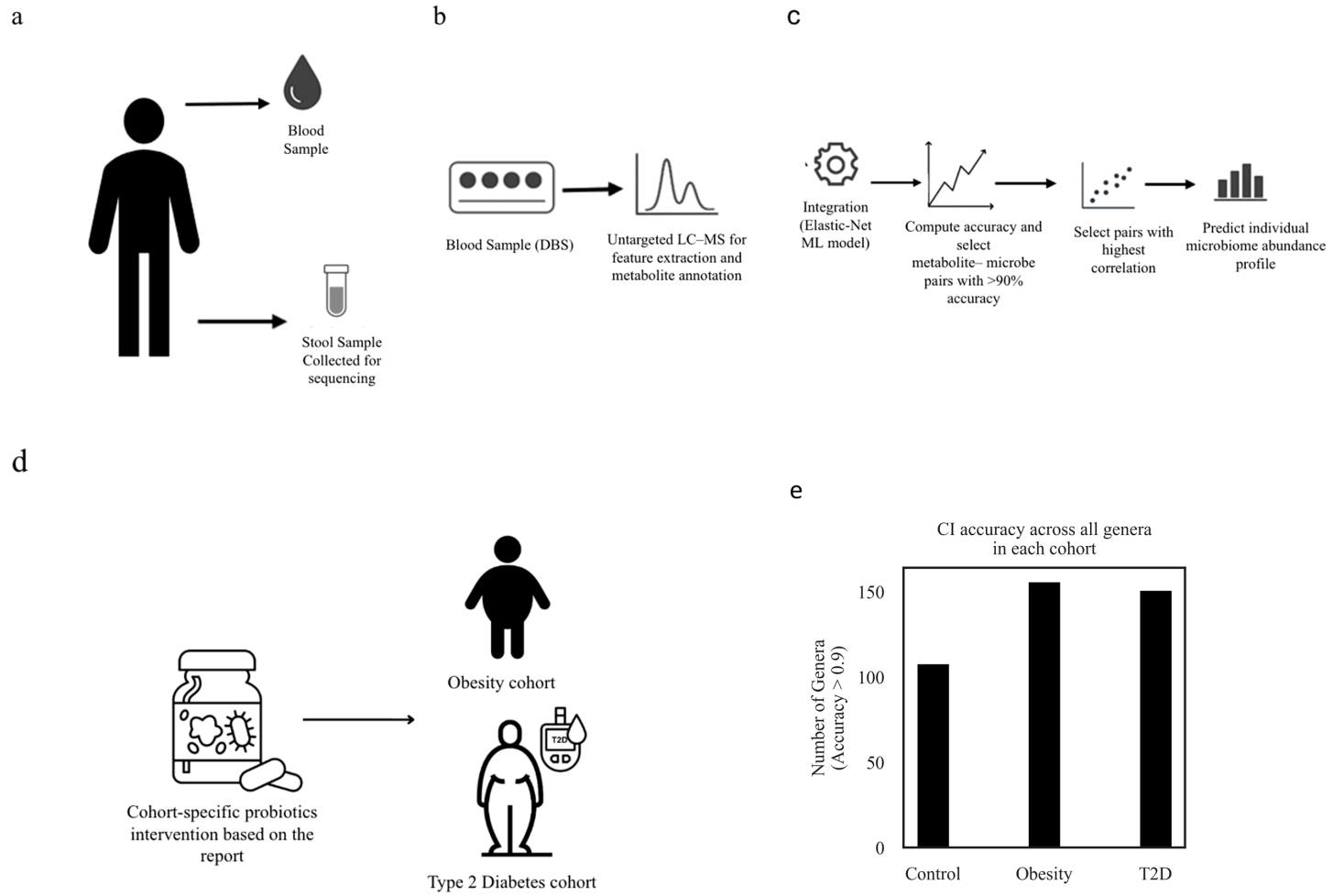


Figure 1

Schematic of study design and the Gut Function Test (GFT) workflow. (a) **Cohorts and samples:** Healthy control, obese, and T2D participants were enrolled. Each subject provided a stool sample and a dried blood spot (DBS). A flow diagram indicates the number of subjects (N) at each stage (Phase 1 profiling and Phase 2 intervention). (b) **Timeline:** Study phases are shown on a timeline. Phase 1 (baseline paired stool–DBS profiling) was followed by Phase 2 (3-month cohort-specific probiotic intervention) with measurements at 0, 1, 2, 3 months. (c) **Metabolomics workflow:** DBS samples were extracted and analyzed by untargeted LC–MS. Metabolite features were detected, aligned, and annotated against spectral libraries. (d) **GFT modeling:**Elastic-Net regression models were trained per microbial genus using the metabolite features as inputs. An example output plot is shown for a representative genus: the red dot is the predicted abundance, the red vertical bar is the 95% confidence interval (CI) around the prediction, and the gray box is the observed abundance (the 95% empirical interval). (e) **Model**

performance: Distribution of CI accuracy (percentage of predictions within the observed 95% CI) for all genera, shown separately for each cohort (Control, Obesity, T2D). The plot highlights high-performing genera (e.g., *Akkermansia*, *Butyrivibrio*) and lower-performing ones (e.g., *Prevotella*).

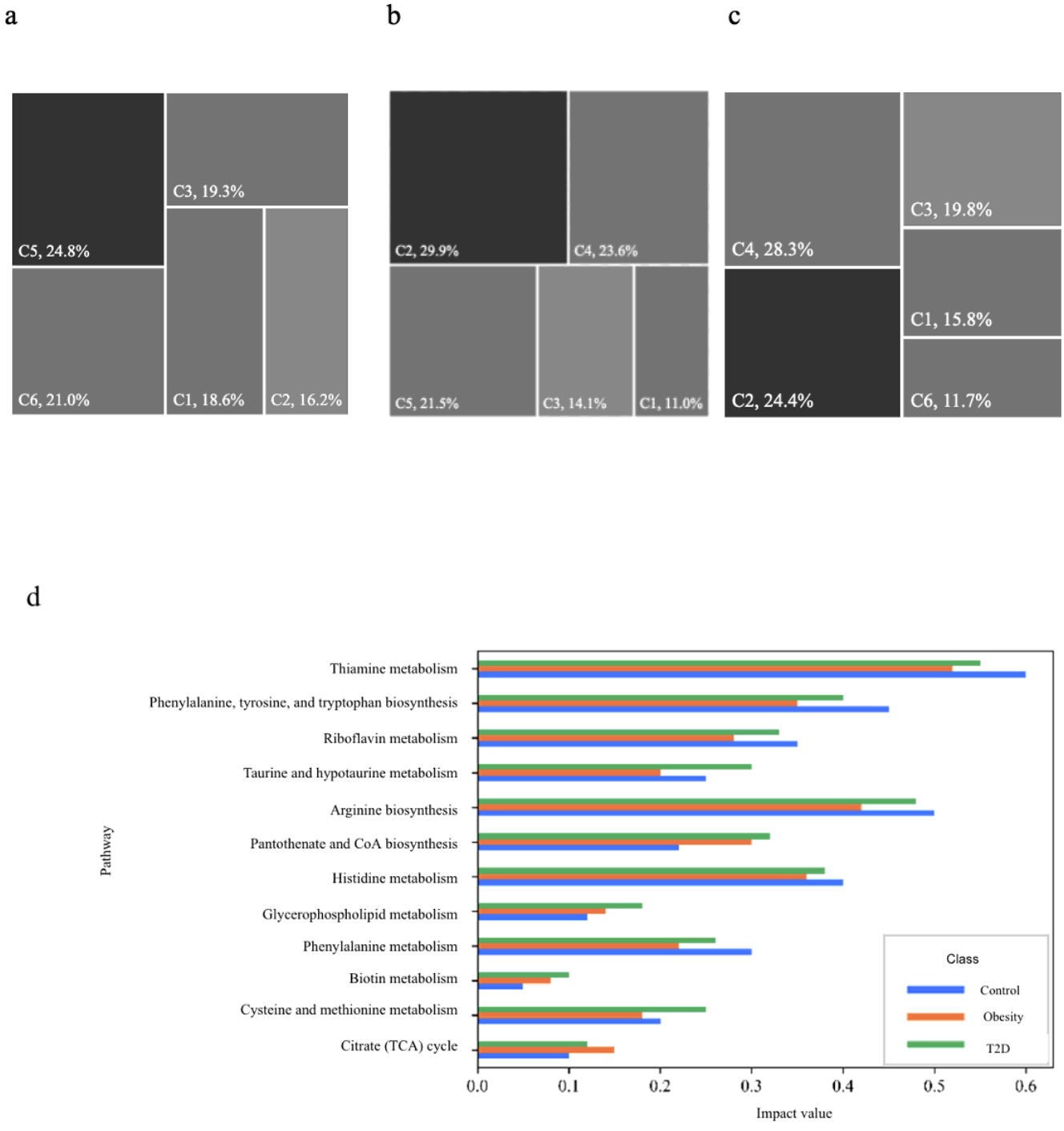


Figure 2

Metabolomic profiles and pathway enrichment across cohorts (Phase 1 data). (a–c) **Metabolite class abundance:** For each cohort (Control, Obesity, T2D), the five most abundant chemical classes of blood metabolites are displayed. Each box represents a chemical class, with box size and shading (darker =

higher) indicating relative abundance. Classes are labeled C1–C6 as follows: C1 = Benzene and derivatives; C2 = Carboxylic acids; C3 = Fatty Acyls; C4 = Organonitrogen compounds; C5 = Organo-oxygen compounds; C6 = Steroids and derivatives. (d) **Pathway enrichment analysis:** Bar chart of the top 10 metabolic pathways that are differentially enriched across the cohorts. Bar length is the enrichment impact score; color indicates pathway category (e.g., green = amino-acid metabolism, blue = lipid metabolism, orange = carbohydrate, etc.). Error bars show 95% confidence intervals for the enrichment scores. Amino-acid metabolic pathways (e.g., BCAA degradation, tryptophan metabolism) are among the top hits.

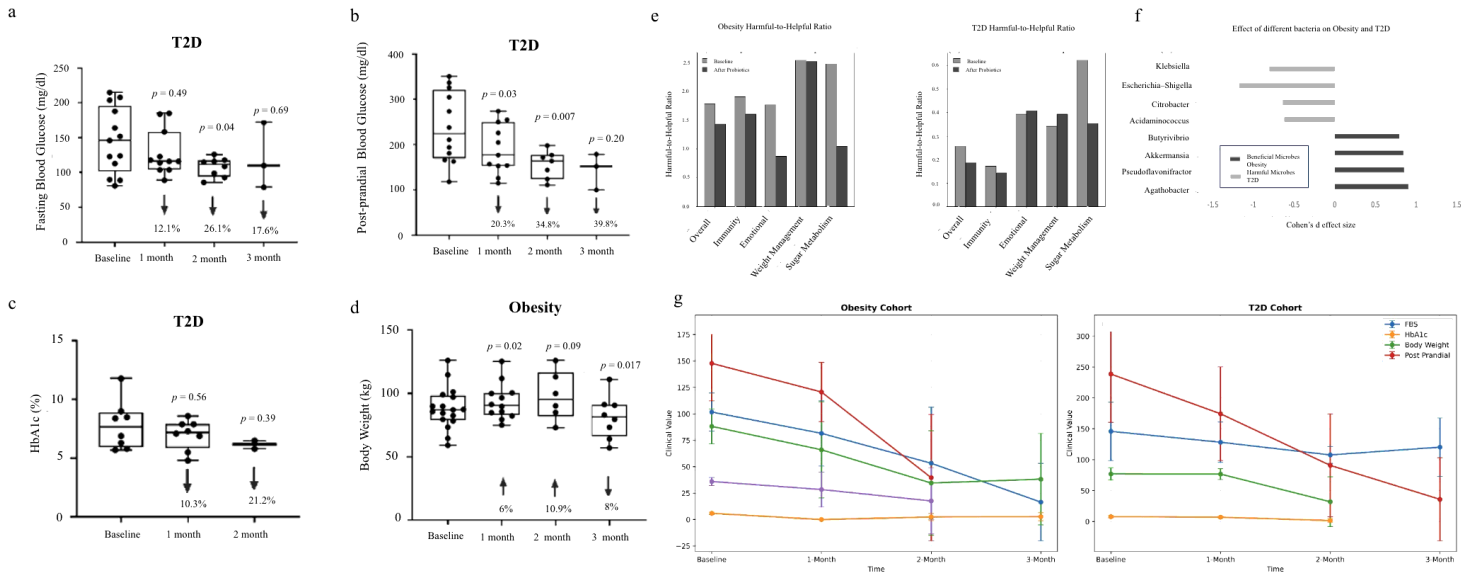


Figure 3

Results of 3-month probiotic intervention in T2D and obesity cohorts. (a) **Fasting blood glucose (FBG)** in the T2D cohort at baseline and monthly follow-ups (n=12). (b) **Postprandial glucose (PPBG)** in T2D over time (n=12). (c) **HbA1c (%)** in T2D at baseline and month 3 (n=12). (d) **Percent body weight change** in the obesity cohort from baseline to month 3 (n=12). In panels (a–d), box plots show the median and interquartile range (IQR), whiskers extend to 1.5× IQR, and individual subjects are overlaid as points (jittered). Asterisks indicate significant change versus baseline (repeated-measures ANOVA with Dunnett's multiple comparisons: *p<0.05, **p<0.01). (e) **Predicted microbiome 'harmful-to-beneficial' ratio**pre- vs post-intervention. A higher ratio indicates a more pathogenic profile. Box plots show median±IQR, 95% confidence intervals, and individual paired values. Post-intervention, this ratio significantly decreased, reflecting predicted gain in beneficial taxa. (f) **Effect sizes (Cohen's d)** for selected genera (post-intervention minus pre-intervention). Positive values indicate increased relative abundance after treatment; negative values indicate decreases. Bars represent Cohen's d; error bars are 95% CIs. Notably, beneficial SCFA-producers (e.g., *Butyrivibrio*, *Akkermansia*) have positive d, while opportunistic pathogens (e.g., *Klebsiella*, *Escherichia–Shigella*) have negative d. (g) **Correlation of microbiome shift with clinical change:**Scatter plot of individual changes in the microbiome ratio (Δ harmful/beneficial) versus change in a clinical outcome (e.g. percent weight change). Each point is one

subject; the Pearson R and p-value are shown. A negative correlation indicates that greater microbiome improvement accompanies greater clinical improvement.

Supplementary Files

This is a list of supplementary files associated with this preprint. Click to download.

- S1R.tiff
- S2.tiff
- S3.tiff
- S4.tiff
- S5.tiff
- S6R.tiff
- TableS1.docx
- SuppLegends.docx